Parity non-conservation effects in atoms

V. A. Alekseev, B. Ya. Zel'dovich, and I. I. Sobel'man

P. N. Lebedev Institute of Physics, USSR Academy of Sciences
Usp. Fiz. Nauk **118**, 385–408 (March 1976)

The possibility is discussed of detecting P-odd weak interaction of the electrons with the nucleus from effects of interaction of atoms with resonance radiation. The requirements of accuracy of three types of experiments are discussed: 1) directly measuring the difference of absorption cross sections for right-hand- and left-hand-polarized light; 2) measuring rotation of the plane of polarization; and 3) measuring the splitting of the intrinsic frequencies of an optical resonator. The calculated values of the expected effect are tabulated for the atoms that are most promising from the experimental standpoint, together with other spectroscopic characteristics of the transition.

CONTENTS

1. INTRODUCTION

The first attempts to detect manifestation of the weak interaction of electrons with nucleons in atomic physics date back to the middle thirties. Thus, they suggested in[1,2] the existence of a weak contact interaction $V = f\delta(r)$, where $\delta(r)$ is the delta function, and they tried to estimate the possible value of the constant f from experimental data on scattering of slow neutrons and on the isotopic shift. They showed that an interaction with a constant f of the order of the Fermi constant $f \sim G_F \approx 10^{-49}$ erg · cm³ might lead only to slight corrections on the background of the rather large theoretical and experimental uncertainties of the measured quantities. Hence it proved possible to give from neutron-scattering data and from the isotropic shift only a very crude upper estimate $f \lesssim 10^{-43}$ erg · cm³, which is 10^6 times the size of the Fermi constant G_F.

After a universal theory of the weak interaction as effected by charged currents had been created, the possibility of detecting effects of the weak interaction in atoms began to seem quite unrealistic. According to this theory, effects that are first-order in G_F are quite impossible, since the matrix elements of interaction for states having a fixed number of electrons are zero.

Only in 1959 was attention called[3] to certain new aspects of the problem. If we assume an interaction of the electrons with the nucleons of the nucleus that is effected by neutral currents and does not conserve parity, in addition to the weak interaction that causes beta decay, then qualitatively new effects arise that involve mixing of even and odd atomic states. Consequently, the emission that corresponds to a series of atomic transitions, in particular the $2s-1s$ transition of the hydrogen atom, must be partially circularly polarized. Moreover, this study showed that rotation of the plane

of polarized light in isotropic media must occur for the same reason. Effects of non-conservation of parity with regard to the hydrogen atom were treated somewhat later.[4]

Interest in the possibility of observing such effects has recently risen considerably,[5–10] both in connection with the progress of the general theory of weak interactions that predicts the existence of neutral currents, and owing to the detection of neutral currents in neutrino experiments. In addition, the development of a new experimental technology based on laser light sources has substantially expanded the possibilities of observing various subtle effects in atomic physics.

The first sufficiently realistic variant of a laser experiment has been treated in[5]. If one excites a Cs atom with a circularly polarized light beam to the $7s$ state ($6s_{1/2}-7s_{1/2}$ transition), and then records the photons emitted in the allowed $7s-6p$ transition, then in principle one can detect the difference between the absorption cross sections σ_+ and σ_- for right-hand and left-hand circular polarization that arises from mixing of s- and p-states. From the estimates of[5], the expected size of the effect is $\Delta\sigma/\sigma \sim 10^{-4}$.

The possibility was treated in[9] of another experiment to detect rotation of the plane of polarization in thallium vapor at a frequency ω close to the resonance ω_0 that corresponds to the magnetic-dipole transition $6p\,{}^2P_{1/2}$, $6p\,{}^2P_{3/2}$. Under favorable conditions (pressure ~ 100 Torr and $\omega - \omega_0 \sim \Delta\omega_D$, where $\Delta\omega_D$ is the Doppler width), the expected effect can amount to $\sim 10^{-7}$ radians/cm. While the discussed effects of non-conservation of parity are small, both of these estimates show that quite realistic hopes yet exist of detecting them.

It seems highly important to the success of the pertinent experiments to choose the optimal objects of study

and experimental scheme. We are considering both the atomic transitions themselves and their amenability to existing lasers, the necessary parameters of the lasers for concrete experimental schemes, etc. This article is specifically concerned with discussing these problems.

Chapter 2 briefly discusses the effect of odd interaction of atomic electrons with the nucleus on the optical characteristics of atomic systems.

Chapter 3 is concerned with choosing optical objects of study, i.e., choosing concrete atomic transitions for which the expected effects are maximal, and which can satisfy a number of demands made by the experimental possibilities. The necessary calculations and estimates are performed, with the details of the calculations deferred to Appendices I–III.

Chapter 4 discusses concrete possible experimental schemes and the parameters and characteristics of lasers that are needed for each of these schemes.

The entire treatment is restricted to optical effects in neutral atoms. Other possible manifestations of non-conservation of parity due to neutral currents, in particular in multiply-charged atoms and in mesonic atoms, are discussed in detail in the review[11].

In making concrete estimates, we shall start with the same expression for the P-odd and T-invariant Hamiltonian V as was used, e.g., in[5, 9]:

$$V = -\frac{Gh^3}{2\sqrt{2}\,c^2 m} Zq\,[(\sigma p)\,\delta(r) + \delta(r)\,(\sigma p)] \,. \tag{1.1}$$

Here G is the Fermi constant, $G = 10^{-5}/m_p^2$, where m_p is the mass of a proton, c is the speed of light, m is the mass of an electron, Z is the charge of the nucleus, $\sigma/2$, p, and r are the spin, momentum, and coordinate of the electron, and the factor $q \approx -0.9$ (see Appendix I).

2. OBSERVABLE EFFECTS

Let us consider the effect of the odd interaction V of the atomic electrons with the nucleus on radiative transitions. Of greatest interest are the optically forbidden transitions between states having the same parity $i \to f$, for which the matrix elements of the electric dipole moment are zero. Here the corrections arising from the potential V will be greatest. Let V^e and V^m be the operators for electric and magnetic dipole transitions. To the level of first-order terms in V, the matrix element of the radiative transition $i \to f$ has the form

$$H'_{if} = V^m_{if} + \sum_k \left(\frac{V_{ik}V^e_{kf}}{\Delta E_{ik}} + \frac{V^e_{ik}V_{kf}}{\Delta E_{fk}} \right) . \tag{2.1}$$

Here $\Delta E_{ab} = E_a - E_b$ is the energy difference between atomic levels, and the summation over k is taken over all states of parity opposite to that of the states i and f.

The circular components of the electric and magnetic field intensities E_ξ and H_ξ are connected by the relationship $E_\xi = -i\xi H_\xi$, where ξ adopts the values $+1$ and -1 for right-hand and left-hand polarizations. Therefore, for the case of emission or absorption of circularly-polarized photons, $V^e_\xi \sim D_\xi E^*_\xi$, and $V^m \sim M_\xi H^*_\xi = +i\xi M_\xi E_\xi$,

where D and M are the operators for the electric and magnetic dipole moments. Upon considering that the matrix V is diagonal in the overall moment J of the atom and in its z-component m, we easily obtain

$$H'_{if} \infty (-1)^{J_i - m_i} \begin{pmatrix} J_i & 1 & J_f \\ -m_i & \xi & m_f \end{pmatrix}$$

$$\times \left\{ (i \| M \| f) + i\xi \sum_k \left[\frac{V_{ik}}{\Delta E_{ik}} (k \| D \| f) - (i \| D \| k) \frac{V_{kf}}{\Delta E_{kf}} \right] \right\} . \tag{2.2}$$

Here

$$\begin{pmatrix} J_i & 1 & J_f \\ -m_i & \xi & m_f \end{pmatrix}$$

is the $3j$-symbol, and $(a \| M \| b)$ and $(a \| D \| b)$ are the reduced matrix elements of M and D. Let us write (2.2) in the form

$$H'_{if}(\xi) \infty \sqrt{S_m(if)}\,(1 + \xi\chi), \tag{2.3}$$

$$\chi = \sum_k \chi_k, \quad \chi_k = i\frac{\beta(i, k)\,(k \| D \| f) - (i \| D \| k)\,\beta(k, f)}{\sqrt{S_m(if)}} , \tag{2.4}$$

$$\beta(a, b) = \frac{V_{ab}}{\Delta E_{ab}} . \tag{2.5}$$

Here $S_m(if) = |(i \| M \| f)|^2$ is the strength of the magnetic dipole-transition line, and $\beta(a, b)$ is the mixing coefficient of the states a and b that arises from the interaction V. To the level of terms linear in χ, we have

$$|H'_{if}(\xi)|^2 \infty S_m(if)\cdot(1 + 2\xi\,\text{Re}\,\chi), \quad \xi = \pm 1. \tag{2.6}$$

As we show in Appendix I, the parameter χ is purely real. Therefore we shall omit the symbol Re henceforth. One can show that the fact that χ is real involves the T-invariance of the Hamiltonian of (1.1), i.e., invariance with respect to time inversion. For a P- and T-odd interaction, the parameter χ would be purely imaginary, and the effects to be discussed in this article would be lacking. Let us denote by σ_ξ and W_ξ the absorption cross section and the probability of emission of a circularly polarized photon, $\Delta\sigma = \sigma_+ - \sigma_-$, and $\Delta W = W_+ - W_-$. Then

$$\frac{\Delta\sigma}{\sigma} = \frac{\Delta W}{W} = 4\chi \,. \tag{2.7a}$$

Here σ and W correspond to $V = 0$, i.e., to the first term in (2.1). Often one introduces the degree of circular polarization P:

$$P = \frac{W_+ - W_-}{W_+ + W_-} = \frac{1}{2}\frac{\Delta W}{W} = 2\chi. \tag{2.7b}$$

However, we shall use the quantities of (2.7a).

Owing to the difference in the absorption cross sections σ_+ and σ_-, a difference also arises in the values of the dielectric constant for right-hand and left-hand circularly polarized waves: $\Delta\varepsilon = \varepsilon_+ - \varepsilon_-$. Let us denote by ε_0 the fraction of the dielectric constant that arises from all the other atomic transitions except for the transition $i \to f$. Since $\varepsilon(\omega) - \varepsilon_0(\omega) \sim \sigma$, we easily obtain

$$\Delta\varepsilon = (\varepsilon - \varepsilon_0)\frac{\Delta\sigma}{\sigma} = (\varepsilon - \varepsilon_0)\cdot 4\chi. \tag{2.8}$$

Thus one can detect the existence of a weak interaction V that violates the law of conservation of parity, either from the difference of absorption cross sections and emission probabilities of circulary-polarized photons, or from the difference between the real parts of ε_+ and ε_-.

3. CHOICE OF ATOMIC TRANSITIONS

The values of $\Delta\sigma/\sigma$ and $\Delta\varepsilon$ from (2.7) and (2.8) depend substantially on the choice of concrete atomic transitions. According to (2.4) and (2.7), $\Delta\sigma/\sigma \propto 4\beta D/M$. Hence it is desirable to achieve the largest values of β and of D, and the lowest possible values of M at which the studied transition could yet be observable. As for the quantities $\mathrm{Re}(\varepsilon_+ - \varepsilon_-)$, transitions are advantageous here that have relatively large values of M (see[9]). However, as we show in Chap. 4, for large enough $M \gtrsim 2\times10^{-2}\,\mu_B$, where μ_B is the Bohr magneton, the observable effects under optimal conditions are proportional to βD, and hardly depend on M.

A. The mixing coefficients β

Let us first examine what are the atomic parameters on which depend the coefficients β from (2.5) for mixing of states of different parity. The calculations of the matrix elements of V are contained in Appendices I and II. Let us use the results of these calculations. In the simplest case of a one-electron atom (one electron outside the filled shells), the operator of (1.1) mixes only s and p states. Here $(s_{1/2}|V|p_{1/2}) \sim R_s^*(0)(R_p/r)_{r\to0}$, where R_s and R_p are the radial functions of the s and p states. The simplest and most reliable way to determine $R_s(0)$ and $(R_p/r)_{r\to0}$ is that adopted in the theory of experimental values of the binding energy of an s-electron and $(R_p/r)_{r\to0}$ in terms of the fine splitting of the levels $p_{1/2}$ and $p_{3/2}$ (see, e.g.,[12]). Consequently we can derive (see (I.26))

$$\beta(s_{1/2}, p_{1/2}) = \frac{\langle s_{1/2}|V|p_{1/2}\rangle}{\Delta E(s_{1/2}, p_{1/2})}$$

$$= i\frac{1}{\pi}\cdot10^{-5}\left(\frac{m}{m_p}\right)^2 \alpha q Z^2 \frac{1}{(n_*^s)^{3/2}}\left(\frac{3\zeta_p}{2\,\mathrm{Ry}}\right)^{1/2}\lambda_{\mathrm{rel}}(Z)\frac{\mathrm{Ry}}{\Delta E(s_{1/2},\,p_{1/2})}.$$

$$(3.1)$$

Here Z is the charge of the atomic nucleus, $\alpha = 1/137$, n_*^s is the effective principal quantum number in the s-state; $3\zeta_p/2$ is the fine splitting of the $p_{1/2}$ and $p_{3/2}$ levels; $\lambda_{\mathrm{rel}}(Z)$ is the relativistic factor of (I.21); and Ry is the Rydberg energy unit.

For polyelectronic atoms, the matrix element of the Hamiltonian of (1.1) differs from zero only for mixing of configurations a and b that contain s and p electrons, respectively. Here

$$\langle a|V|b\rangle = \langle s_{1/2}|V|p_{1/2}\rangle Q(a, b), \qquad (3.2)$$

where Q is a factor of the order of unity that depends on the angular momenta. Formulas for the factors Q are given in Appendix II.

It is interesting to discuss the dependence of the mixing coefficient β on the nuclear charge Z. The fine-splitting parameter of the p-level $\zeta_p \propto Z^2(n_*^p)^{-3}$. Hence the coefficient $\beta \propto Z^3\lambda_{\mathrm{rel}}(Z)(n_*^p\,n_*^s)^{-3/2}(\Delta E(s,p))^{-1}$. For $Z \lesssim 30$, $\lambda_{\mathrm{rel}}(Z) \approx 1$, while for $Z \gtrsim 40$, $\lambda_{\mathrm{rel}}(Z)$ increases rapidly with increasing Z and reaches a value $\lambda_{\mathrm{rel}} = 6$ at $Z = 80$. We can assume that the principal quantum numbers $n_*^{s,p}$ and the energy differences $\Delta E(s, p)$ do not depend on Z.[1] Therefore the mixing coefficients β increase with increasing Z as Z^3 for $Z \lesssim 30$, and somewhat more rapidly than Z^3 for $Z \gtrsim 30$. Thus the greatest

values of β are realized in the heavy atoms. This important circumstance was first noted in[5].

B. Matrix elements of the magnetic dipole M

In the non-relativistic approximation, the matrix elements of the magnetic dipole differ from zero only for transitions between the fine-structure components of a single term or the hyperfine-structure components of a single level. All the matrix elements of this type are equal in order of magnitude to the Bohr magneton μ_B. For transitions between levels of differing electronic configurations or between different LS terms, the matrix elements of M in the non-relativistic approximation are zero. Mixing of electronic configurations caused by electrostatic interaction of electrons does not relax this rule. The rule is relaxed only by relativistic effects. Two types of such effects can occur: relativistic corrections to the magnetic-moment operator[13] and either spin-orbit interaction or a joint influence of mixing of configurations and spin-orbit interaction.

Let us start with the first of these effects. When we take account of the higher terms in the expansion in terms of v/c (v is the velocity of the electron) in the operator M, additional terms M' arise that are of the order of α^2: $\mathrm{M} = \mu_B(\sigma+1)+\mathrm{M}'$. For $ns_{1/2}-n's_{1/2}$ transitions in the hydrogen atom,

$$\mathrm{M}' = -\mu_B\sigma\cdot\frac{1}{3}\frac{\alpha^2}{\mathrm{Ry}}\frac{\mathbf{p}^2}{2m}. \qquad (3.3)$$

For $ns_{1/2}-n's_{1/2}$ transitions in alkali atoms.[6]

$$\mathrm{M}' = -\mu_B\sigma\cdot\frac{1}{3}\frac{\alpha^2}{\mathrm{Ry}}\left[\frac{\mathbf{p}^2}{2m} + \frac{1}{2}\frac{d}{dr}(rU)\right]. \qquad (3.4)$$

Here $U(r)$ is the effective potential for the valence electron. The second term in (3.4) is substantial only when $r \lesssim r_0$ where r_0 is the radius of the atomic residue, since when $U \propto 1/r$, $d(rU)/dr = 0$. We can easily show that the relative contribution of this term to the matrix element of the transition is small. It may prove necessary to take this term into account in treating transitions between levels for which one of the principal quantum numbers n or n' is large, when the contribution of the first term to (3.4) may prove to be anomalously small. However, we must also take account here of the exchange interaction of the valence electron with the electrons of the filled shells, which gives a contribution of the same order of magnitude as the second term in (3.4). Hence we shall use the expression (3.3) in the estimates below.[2]

The matrix elements of the operator of (3.3) depend

---

[1] Whenever ΔE_{ab} is anomalously small for any reason (e.g., $\Delta E_{ns,np}$ in the hydrogen atom), the mixing coefficient β becomes very large. However, here the studied transition falls on the tail of a strong, optically allowed transition. This makes an experiment to measure the absorption cross-section practically impossible. Experiments of the other types for hydrogen are apparently also unrealistic; see[11].

[2] A detailed derivation of the expression for the magnetic-dipole operator for helium and helium-like ions can be found in[13,14]. However, a generalization of this expression to the alkaline-earth atoms requires that we should also take account of exchange interaction with the inner filled shells.

weakly on Z, and they amount to $\sim 0.1\ \alpha^2\ \mu_B$ for many transitions between ground and lower excited levels, e.g., $ns \rightarrow (n+1)s$ transitions in alkali atoms. Thus, numerical calculations performed with semiempirical wave functions[15] give the following values of the square of the matrix element $|\langle ns|\, p^2/2m\, |n's\rangle|^2$: potassium, $4s-5s-0.1$ Ry^2; rubidium, $5s-6s-0.15$ Ry^2; cesium, $6s-7s-0.2$ Ry^2. As we see, the Z-dependence is actually very weak, at any rate as compared with the $\beta(Z)$ relationship.

Now let us proceed to spin-orbit interaction and mixing of configurations. These effects depend very strongly on Z, while this relationship differs for atoms having the ground configurations ns, ns^2, and np^k.

For atoms having the ground electronic configuration np^k, the transitions of interest are either those between the fine-structure components of the ground term, e.g., $np\,^2P_{1/2}-np\,^2P_{3/2}$, $np^5\,^2P_{3/2}-np^5\,^2P_{1/2}$, $np^2\,^3P_0-np^2\,^3P_1$, etc., or those between the terms of the ground electronic configuration, e.g., $np^3\,^4S_{3/2}-np^3\,^2D_{3/2,5/2}$. $M \sim \mu_B$ for transitions of the first type. In the case of transitions of the second type for $Z \gtrsim 40$, $M \sim (0.1-1)\mu_B$,[16] owing to strong spin-orbital interaction that mixes different SL terms (S is the total spin, and L is the total orbital angular momentum). This is precisely the situation for the bismuth atom that we shall treat below.

For alkaline-earth and alkali elements, the transitions of interest are forbidden $s-s$ transitions that change the principal quantum number: $ns^2\,^1S_0 \rightarrow nsn'\,s\,^3S_1$ and $ns_{1/2} \rightarrow (n+1)s_{1/2}$.

For the alkaline-earth atoms ($ns^2\,^1S_0-nsn's\,^3S_1$ transitions), the selection rule is relaxed by the joint influence of interaction of the configurations ns^2, ns, $n's$ with the pp configuration and spin-orbit interaction. The configuration interaction mixes atomic states of the type

$$\Psi(ns^2\,^1S_0) = a\Psi(ns^2\,^1S_0) + b\Psi(n_1pn'_1p\,^1S_0),$$
$$\Psi(nsn's\,^3S_1) = a'\Psi(nsn's\,^3S_1) + b'\Psi(n_1pn'_1p\,^3S_1). \qquad (3.5)$$

As before, the matrix element M of the transition as taken over these functions is zero, since a magnetic-dipole transition can occur only between states of like spin, even with identical principal quantum numbers. In turn, the spin-orbital interaction in the pp configuration mixes the terms $^1S_0$ and $^3P_0$, $^3S_1$ and $^3P_1$:

$$\Psi(n_1pn'_1p\,^1S_0) = \gamma\Psi(n_1pn'_1p\,^1S_0) + \delta\Psi(n_1pn'_1p\,^3P_0),$$
$$\Psi(n_1pn'_1p\,^3S_1) = \gamma'\Psi(n_1pn'_1p\,^3S_1) + \delta'\Psi(n_1pn'_1p\,^3P_1). \qquad (3.6)$$

Consequently,

$$M = bb'\delta\delta'\,(^3P_0\,\|\,M\,\|\,^3P_1) \approx bb'\delta\delta'\mu_B. \qquad (3.7)$$

The coefficient δ rapidly ($\propto Z^2$) increases with increasing Z. At $Z \approx 40-50$, it attains value $\sim 0.1-0.3$.[12,17] A sufficiently reliable estimate of the coefficients b and b' in (3.6) requires special numerical calculations, since actually it is not a single close-lying pp state that is effectively admixed in (3.5), but a large number of such states from both the discrete and the continuous spectrum. According to[18], throughout the series of atoms having the ground configuration ns^2 from beryl-

lium to mercury, the overall mixing coefficient of all the pp and p^2 states is $0.2-0.35$, without any regular dependence on Z. We can naturally assume that the contribution of the close-lying pp configurations for which δ is largest is no less than 0.1. Hence the factor $bb'\delta\delta'$ rapidly grows from 10^{-4} at $Z \approx 40$ to 10^{-2} for the largest Z values.

The situation is about the same for the alkali atoms, i.e., for atoms having the ground configuration ns. However, here the configurations $p^5npn's$ (see[8]), which correspond to excitation of the closed p^6 shell, are admixed into the configuration p^6ns. Therefore the coefficients b can be somewhat smaller than in the case of mixing of the configurations $ns^2-npn'p$. Figure 1 shows the approximate form of the $M(Z)$ relationship for $ns_{1/2} \rightarrow (n+1)s_{1/2}$ transitions in alkali atoms and $ns^2\,^1S_0 \rightarrow ns(n+1)s\,^3S_1$ transitions in the alkaline-earth atoms.

C. Z-dependence of the quantities $\Delta\sigma/\Delta$ and $\mathrm{Re}\,(\epsilon_+ - \epsilon_-)$

The matrix elements of D for neutral atoms are practically independent of Z. Hence Z-dependence of the quantity $\Delta\sigma/\sigma \sim \beta D/M$ is determined by the form of $\beta(Z)$ and $M(Z)$. Figure 1b shows the approximate Z-dependence of $\Delta\sigma/\sigma$ for $ns_{1/2}-(n+1)s_{1/2}$ transitions in alkali atoms and $ns^2\,^1S_0-ns(n+1)s\,^3S_1$ transitions in alkaline-earth atoms. At first, $\Delta\sigma/\sigma$ rises rapidly with increasing Z, just like $\beta(Z)$; then this growth becomes saturated, since the dependence $M \propto Z^4$ begins to be manifested at large Z.

All the above-said implies that the largest values of $\Delta\sigma/\sigma$ in the studied strongly forbidden transitions are realized at $Z > 30-40$. Yet the matrix elements M for these transitions that determine the absorption cross sections σ themselves are very small, $\sim 10^{-4}\ \mu_B$. Therefore it is hardly expedient to try to increase $\Delta\sigma/\sigma$ by further decrease in M. In principle one can point out transitions for which $M < 10^{-5}\ \mu_B$, e.g., transitions from an $ns_{1/2}$ ground state to a strongly excited $n's_{1/2}$ state. Yet it is practically impossible to detect the absorption from such transitions because it will overlap the absorption in the tail of the allowed absorption $ns_{1/2}-n'p_{1/2,3/2}$.
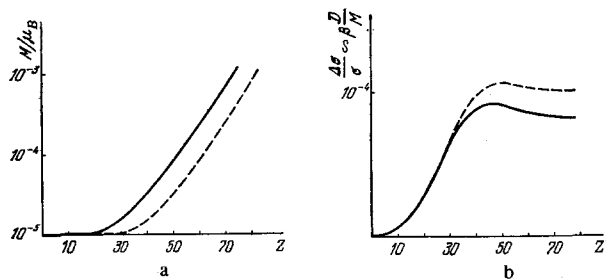

FIG. 1. (a) relationship between the matrix element M of the magnetic-dipole transition and the nuclear charge Z (solid line—$ns^2\,^1S_0 \rightarrow ns(n+1)s\,^3S_1$ transition in alkali-earth atoms, dotted line—$ns\,^2S_{1/2} \rightarrow (n+1)s\,^2S_{1/2}$ transition in alkali atoms); (b) relationship between the relative difference in cross sections $\Delta\sigma/\sigma$ and the nuclear charge Z (as in Fig. 1(a), the solid and dotted lines correspond to $ns^2\,^1S_0 \rightarrow ns(n+1)s\,^3S_1$ and to $ns\,^2S_{1/2} \rightarrow (n+1)s\,^2S_{1/2}$ transitions, respectively).

Element	Transition	ν, cm^{-1}	λ, μm	s_m	W, sec^{-1}	σ, cm^2	$\Delta\sigma/\sigma = \Delta W/W$
	Configuration ns						62
Rb$_{85}^{37}$	$6s_{1/2} \to 5s_{1/2}$	20 133.6	0.496 682	10^{-8}	$1.1 \cdot 10^{-6}$	$6.9 \cdot 10^{-26}$	$1.13 \cdot 10^{-4}$
Cs$_{33}^{55}$	$7s_{1/2} \to 6s_{1/2}$	18 535.51	0.539 505	10^{-8}	$8.6 \cdot 10^{-7}$	$9.6 \cdot 10^{-26}$	$5.7 \cdot 10^{-4}$
	Configuration ns^2						
Sr$_{88}^{38}$	$5s6s{}^3S_1 \to 5s^2\,{}^1S_0$	29 038.795	0.344 366	10^{-8}	$2.22 \cdot 10^{-6}$	$1.41 \cdot 10^{-25}$	$3.0 \cdot 10^{-4}$
Ba$_{137}^{56}$	$6s7s{}^3S_1 \to 6s^2\,{}^1S_0$	26 160.284	0.382 259	10^{-5}	$1.6 \cdot 10^{-3}$	$1.74 \cdot 10^{-22}$	$1.8 \cdot 10^{-5}$
Hg$_{200}^{80}$	$6s7s{}^3S_1 \to 6s^2\,{}^1S_0$	62 350.456	0.160 384	10^{-5}	$6.7 \cdot 10^{-2}$	$6.5 \cdot 10^{-22}$	$1.7 \cdot 10^{-5}$
	Configuration np^k						
I$_{127}^{53}$	$5p^5\,{}^2P_{1/2} \to 5p^5\,{}^2P_{3/2}$	7 603.15	1.315 244	4/3	8	$5.6 \cdot 10^{-18}$	$1 \cdot 10^{-8}$
Tl$_{204}^{81}$	$6p\,{}^2P_{3/2} \to 6p^2P_{1/2}$	7 792.7	1.283 26	4/3	4.33	$1.4 \cdot 10^{-17}$	$2.6 \cdot 10^{-7}$
Pb$_{207}^{82}$	$6p^2\,{}^3P_1 \to 6p^2\,{}^3P_0$	7 819.85	1.278 879	2	8.6	$4.3 \cdot 10^{-17}$	10^{-6}
Bi$_{209}^{83}$	$6p^3\,{}^2P_{1/2} \to 6p^3\,{}^4S_{3/2}$	21 661.0	0.461 659	0.4	56	$2.25 \cdot 10^{-18}$	
	$6p^3\,{}^2P_{3/2} \to 6p^3\,{}^4S_{3/2}$	33 164.84	0.301 524 14	0.035	8.74	$0.2 \cdot 10^{-18}$	$1 \cdot 10^{-6}$
	$6p^3\,{}^2D_{3/2} \to 6p^3\,{}^4S_{3/2}$	11 419.03	0.875 731 1	1.65	16.7	$9.0 \cdot 10^{-18}$	
	$6p^3\,{}^2D_{5/2} \to 6p^3\,{}^4S_{3/2}$	15 437.66	0.647 766	0.35	5.8	$1.3 \cdot 10^{-18}$	

The most suitable atoms for experiments to measure $\mathrm{Re}(\varepsilon_+ - \varepsilon_-)$ are the heaviest of the atoms having np^k configurations, for which there is an entire series of transitions in the visible and the near infrared having $M \sim (10^{-2}-1)\mu_B$, as was first noted in[9].

D. Results of calculations

The table gives the characteristics of a series of transitions in atoms having the ground-state configurations ns, ns^2, np, np^2, and np^5, as well as the results of the performed calculations of the parameter $\Delta\sigma/\sigma$ $= \Delta W/W$. The conduct of these calculations is based on highly varied spectroscopic information on the atoms and on concrete transitions. The corresponding information is given in Appendix III, together with a discussion of the applied approximations. The probability W of magnetic-dipole transition that is given in the table is calculated by the formula

$$W = \frac{4}{3}\frac{\omega^3}{\hbar c^3}\frac{1}{g_f}\left(\frac{e\hbar}{2mc}\right)^2 s_m \ .$$

Here g_f is the statistical weight of the upper state, and s_m is the strength of the line, which is also given in the table, as expressed in Bohr magnetons: $|(i \,\|\, M \,\|\, f)|^2$ $= S_m = s_m(e\hbar/2mc)^2$. This probability corresponds to the overall probability of transition from an arbitrary hyperfine sublevel of the upper state to all the hyperfine sublevels of the lower state. The absorption cross-section of interest to us for a magnetic-dipole transition with an electric dipole admixture at the frequency ω is:

$$\sigma_\pm(\omega) = \left(1 \pm \frac{1}{2}\frac{\Delta W}{W}\right)\sigma(\omega) \ . \tag{3.8}$$

Here $\sigma(\omega)$ is the cross section for the magnetic-dipole transition with account taken of the hyperfine and isotopic structure of the line, as well as of Doppler and collision broadening. Thus the ratio $\Delta\sigma(\omega)/\sigma(\omega) = \Delta W/$

W does not depend on the factors that broaden and split the line.[3]

The hyperfine and isotopic structure were not taken into account in calculating the cross-section σ given in the table. This elevates of the calculated cross section as compared with that at the maximum of the most intense hyperfine component by a factor of 1.5–2. The value of σ given in the table is calculated for the center of the Doppler-broadened line by the formula

$$\sigma = \frac{1}{8\pi\sqrt{2\pi}}\frac{W}{\nu^3}\sqrt{\frac{M}{kT}}\frac{g_f}{g_i}$$

(where M is the mass of the atom) at a temperature $T = 1000\,^\circ\mathrm{K}$. For iodine, thallium, lead, and bismuth, the magnetic-dipole transition is allowed, and the strength s_m of the line is calculated exactly.[4] In the atoms of rubidium, strontium, cesium, barium, and mercury, the strength s_m of the line was estimated very approximately with account taken of configuration-interaction effects. Experimental measurements would be very desirable for the line strengths of these transitions, which could alter the size of the effect $\Delta\sigma/\sigma$ given in the table by a factor equal to $\sqrt{s_m^{\mathrm{tab}}/s_m^{\mathrm{exp}}}$.

4. POSSIBLE EXPERIMENTAL SCHEMES

A. Measurement of the difference of absorption cross-sections $\sigma_+ - \sigma_-$

As we see from the table, the maximum values of $\Delta\sigma/\sigma$ correspond to very small $\sigma \sim 10^{-25}$ cm^2 at which direct observation of absorption is difficult: the fraction of absorbed photons at a density $N \sim 10^{18}$ cm^{-3} and

---

[3] Whenever an electric quadrupole transition exists simultaneously with the magnetic–dipole transition, Eq. (3.8) loses force.

[4] See[16,17] on the calculation of s_m for bismuth.

cuvette length $L \sim 10$ cm is $N\sigma L \sim 10^{-4}$. In[5] they proposed measuring the quantities σ_+ and σ_- by recording the number of absorption events via the emission from the excited atoms in an allowed transition to a low-lying level of opposite parity. For the alkali atoms, this would be absorption in an $ns \rightarrow n's$ transition and subsequent emission in an $n's \rightarrow np$ transition; for the alkaline earths, absorption in an $ns^2\,^1S_0 \rightarrow nsn'n\,^3S_1$ transition and emission in an $nsn's\,^3S_1 \rightarrow nsnp\,^3P_1$ transition. Let us examine the requirements imposed on the accuracy of the measurements in this experiment. Let I_1 and I_2 be the photon fluxes for preferential right-hand and left-hand polarization, respectively, the polarization states being fixed with accuracies x_1 and x_2. That is, let the first beam contain a small admixture x_1 of levo-polarized light, and the second an admixture of x_2 of dextro-polarized light, with x_1, $x_2 \ll 1$. If we denote by I'_1 and I'_2 the measured photon fluxes for the allowed transition: $I'_1 = I_1 N\sigma_+ L$, and $I'_2 = I_2 N\sigma_- L$, we obtain for the effect of interest to us:

$$\frac{\sigma_+ - \sigma_-}{\sigma_0} = \left(\frac{I'_1 - I'_2}{I'_1} - \frac{I_1 - I_2}{I_1}\right)(1 - x_1 - x_2)^{-1}. \qquad (4.1)$$

We see from (4.1) that the requirements imposed on the purity of polarization of the beams are not large: it quite suffices to have x_1, $x_2 \lesssim 10^{-2}$, which causes no difficulties. Hence the sensitivity of the method with respect to measuring the small quantities $(\sigma_+ - \sigma_-)/\sigma$ is determined to the same accuracy as that to which one can measure $(I_1 - I_2)/I_1$ and $(I'_1 - I'_2)/I'_1$.

Two variants of the experiment are possible: 1) successively turning on the beams I_1 and I_2, and 2) simultaneously exposing two portions of the volume of the cuvette.

In the former case, we must monitor the frequency of the exciting radiation, since deviations of the frequency by $\delta\omega$ from the center of the line will diminish the absorption cross-section by the amount $\Delta\sigma = (\delta\omega/\Delta\omega_D)^2 \sigma$, where $\Delta\omega_D$ is the Doppler width of the line. Hence we must have $\delta\omega \ll \Delta\omega_D \sqrt{\Delta\sigma/\sigma}$. The splitting by the magnetic field also must not exceed $\Delta\omega_D\sqrt{\Delta\sigma/\sigma}$. This leads to the requirement that $H \ll 10^2 \sqrt{\Delta\sigma/\sigma}$Oe.

In the latter case, large fluctuations $\delta\omega$ are admissible. If these fluctuations are actually large, then the requirements for eliminating magnetic fields become stricter: $H \ll 10^2(\Delta\omega_D/\delta\omega)(\Delta\sigma/\sigma)$ Oe.

The requirements on the admissible stray electric fields make no serious difficulties (see[5]).

Let us estimate typical values of the measured fluxes I'_1 and I'_2. We shall assume that the collision width does not exceed $\Delta\omega_D$ for the chosen N. Then the probability of quenching of the excited state is substantially smaller than that of the allowed optical transition. Hence the yield of luminescence photons is $Q \approx I\sigma N$, and $I' \approx I\sigma NL$, where L is the linear dimension of the exposed volume. For $N \approx 10^{18}$ cm^{-3}, $\sigma \approx 10^{-25}$ cm^2, which corresponds to the minimum value of σ in the table, $Q \approx 10^{-7}I$. If we use a cw laser as the excitation source, then we must orient ourselves to fluxes $I \sim 10^{17}$ cm^{-2} sec^{-1} (laser power $\sim 10^{-2}$ W with beam diameter ~ 1 cm). Here $Q \sim 10^{10}$ photons/cm^3 sec. With a pulsed laser, we can expect pulses of exciting light of the order of 10^{16}–10^{18} photons (energy 10^{-3}–10^{-1} J) and luminescence pulses of the order of 10^9–10^{11} photons. The luminescence yield is large enough in both cases.

A concentration of vapors of alkali and alkaline-earth atoms of $N \sim 10^{18}$ cm^{-3} can be obtained only at relatively high temperatures $T \sim 700$–1500 °K. One must consider at such temperatures the possible onset of thermal emission at the luminescence frequency from the gas being studied. In order to estimate the role of this effect, it suffices to compare the thermal population of the excited level $N_2 = Ne^{-\hbar\omega/kT}$ with the population $\Delta N = I\sigma\tau N$ that is produced by the steady-state absorption of quanta from the incident flux of I quanta/cm^2 sec; τ is the radiation lifetime of the excited level, where $\tau \sim 10^{-7}$ sec. Let us give estimates of $\Delta N/N_2$ for the temperature at which the saturated vapor density reaches $N \sim 10^{18}$ cm^{-3}: rubidium—$T \approx 800$ °K, $\Delta N/N_2 = 5 \times 10^{-16}I$; cesium—$T \approx 670$ °K, $\Delta N/N_2 = 2 \times 10^{-15}I$; strontium—$T \approx 1370$ °K, $\Delta N/N_2 = 3 \times 10^{19}I$; barium—$T \approx 1570$ °K, $\Delta N/N_2 \approx 5 \times 10^{-19}I$; mercury—$T \approx 530$ °K, $\Delta N/N_2 \approx 10^{46}I$. Thus, with a continuous laser giving $I \sim 10^{17}$ quanta/cm^2 sec, the thermal background does not exceed the useful signal for mercury, cesium, and apparently rubidium. With a pulsed laser having $I \sim 10^{23}$ quanta/cm^2 sec, the useful signal is larger than or of the order of the thermal background for all the studied elements having a forbidden magnetic-dipole transition. Thermal emission from the walls and windows of the cuvette can also cause substantial difficulties.

One need not use the emission of the excited atoms in an allowed transition in order to detect the difference between the numbers of excitation events by dextro- and levo-polarized light. In principle, other methods are possible. For example, a difference between σ_+ and σ_- leads to a difference between the populations N_+ and N_- of the $\pm m$ components of the excited level, and hence, to a difference between the magnetic moments $N_+\mu_B$ and $N_-\mu_B$ created by irradiating the gas with the light fluxes I_+ and I_-. In detecting $N_+\mu_B$ and $N_-\mu_B$, it is most convenient to use an $ns^2\,^1S_0$–$nsn's\,^3S_1$ transition. This is because the moment of the atom is zero in the ground state, and the thermal fluctuations of the magnetic moment are small. They are determined only by the thermal fluctuations of the populations of the m-components of the excited level.

B. Rotation of the plane of polarization

As we have mentioned in Chap. 2, a difference between the absorption cross sections σ_+ and σ_- leads to a difference between the real parts: $\text{Re}(\varepsilon_+ - \varepsilon_-) \neq 0$, owing to the Kramers–Kronig relationships. This difference can be measured from the angle of rotation of the plane of polarization θ as the light passes through a cuvette of length L containing the studied gas:

$$\theta = \frac{1}{4}\frac{\omega_0}{c} L\,\text{Re}(\varepsilon_+ - \varepsilon_-). \qquad (4.2)$$

As has been shown in[9], transitions having $M \sim \mu_B$ are most suitable for this, i.e., elements having the ground configuration np^k. In frequency regions close to the frequency of the studied magnetic-dipole transition, $\varepsilon(\omega)$

is determined by the convolution of the Doppler and Lorentz contours

$$\varepsilon_{\pm}(\omega) = 1 + N\sigma \frac{c}{\omega_0}\left(1 \pm \frac{1}{2}\frac{\sigma_+ - \sigma_-}{\sigma_0}\right)\frac{1}{\pi}\int \frac{\exp\{-[(\omega'-\omega_0)/\Delta\omega_D]^2\}}{\omega'-\omega-i\gamma}d\omega',$$

$$(4.3)$$

where γ is the collision width. There is no rotation at the center of the line. When $\gamma \ll \Delta\omega_D$, the maximum of the quantity $\mathrm{Re}(\varepsilon_+ - \varepsilon_-)$ is attained when $|\omega - \omega_0| = 0.93\,\Delta\omega_D$ (see the table in[19]). At this point of the contour, the angle θ and the beam attenuation $\exp(-\varkappa L)$ are

$$\theta = -0.61 N\sigma_0 L \frac{\sigma_+ - \sigma_-}{\sigma_0}\frac{\omega-\omega_0}{|\omega-\omega_0|}, \qquad (4.4a)$$

$$\exp(-\varkappa L) = \exp(-0.41 N\sigma_0 L), \qquad (4.4b)$$

where $\varkappa = (\omega/c)\,\mathrm{Im}\,\varepsilon$ is the absorption coefficient. We see from Eq. (4.4) that the rotation angle for a given value of $(\sigma_+ - \sigma_-)/\sigma_0$ is proportional to $N\sigma_0 L$, which also determines the absorption in the distance L. It seems unrealistic to make measurements at an absorption greater than $e^{-10} \approx 4.5\times10^{-5}$. For atoms having the configuration np^k, $\Delta\sigma/\sigma \lesssim 10^{-6}$ (see the table), and $|\theta| \lesssim 7(\sigma_+ - \sigma_-)\sigma_0 \sim 7\times10^{-6}$. It seems to be an extremely hard problem to detect such a small rotation angle. An absorption of e^{-10} corresponds to $N\sigma_0 L = 25$. With a cross section of $\sigma_0 \approx 10^{-17}$ cm² (see the table), this is easily attained at a concentration $N = 10^{18}$ cm⁻³ and $L = 2.5$ cm. Since the length $L = 2.5$ cm can be considerably increased (up to $L \approx 10^2$ cm), one can try to increase the rotation angle by increasing the parameter $N\sigma_0 L$, while eliminating absorption by frequency detuning in the tail of the line, since the absorption declines more rapidly than the dispersion in the tail.

The absorption and the rotation of the plane of polarization in the tail are determined by the dispersion contour of the line at uniform width γ. The size of γ in neutral gases arises from the collision mechanism of broadening caused by the van der Waals interaction, and it is proportional to the density. The van der Waals broadening depends weakly on the concrete type of atoms and the temperature of the gas; usually the width γ is comparable with the Doppler width $\Delta\omega_D$ of the line when $N \approx 10^{18}$ cm⁻³. Hence, in rough estimates we can assume $\gamma \approx \Delta\omega_D N \cdot 10^{-18}$.

In the dispersion tail of the line,

$$\theta = \frac{1}{4\sqrt{\pi}}N\sigma_0 L \frac{\sigma_+ - \sigma_-}{\sigma_0}\frac{\Delta\omega_D}{\omega-\omega_0}, \qquad (4.5)$$

$$\varkappa L = \frac{1}{\sqrt{\pi}}N\sigma_0 L \frac{\gamma}{\Delta\omega_D}\frac{\Delta\omega_D^2}{(\omega-\omega_0)^2}, \qquad \gamma \infty N. \qquad (4.6)$$

If we set again the limiting absorption $\exp(-\varkappa L) = e^{-10}$, we can select an optimal detuning from resonance

$$|\omega - \omega_0| = \Delta\omega_D \sqrt{\frac{N\sigma_0}{\sqrt{\pi}\varkappa}\frac{\gamma}{\Delta\omega_D}} \approx \Delta\omega \sqrt{\frac{N\sigma_0 L}{10\sqrt{\pi}}\frac{\gamma}{\Delta\omega_D}}. \qquad (4.7)$$

With this choice of $|\omega - \omega_0|$, if the condition is satisfied that

$$\frac{N\sigma_0 L}{10\sqrt{\pi}}\frac{\gamma}{\Delta\omega_D} \gg 1, \qquad (4.8)$$

which ensures the inequality $|\omega - \omega_0| \gg \Delta\omega_D$, we get for the angle θ:

$$\theta = \frac{1}{8\pi^{1/4}}\sqrt{10 N\sigma_0 L \frac{\Delta\omega_D}{\gamma}\frac{\sigma_+ - \sigma_-}{\sigma_0}}. \qquad (4.9)$$

Since γ is proportional to the density, the angle θ from (4.9) does not depend on N. Moreover, since $(\sigma_+ - \sigma_-)/\sigma_0 \sim \beta D/M$, while $\sigma_0 \sim M^2$, the angle θ also does not depend on M. We recall that we are speaking of rather large $M \sim \mu_B$, for which $N\sigma_0 L \gg 1$ ($\sigma_0 > 10^{-20}$, $M > 2 \times 10^{-2}\,\mu_B$). Thus, we must achieve the maximum possible values of βD in choosing the concrete transitions. If we substitute into (4.9) typical values of the parameters (see the table): $\sigma = 10^{-17}$ cm², $\Delta\sigma/\sigma = 2\times10^{-6}$, $N = 10^{18}$ cm³ (here $\gamma \approx \Delta\omega_D$), and $L = 100$ cm, we get $\theta \approx 0.25\times10^{-4}$. The necessary frequency detuning in this case is $|\omega - \omega_0| = 10\gamma = 10\,\Delta\omega_D$.

The studied example shows the scale of the effect of rotation of the plane of polarization that we might expect under optimal experimental conditions. Generally the angle θ measured in an actual experiment contains also a contribution from the uneliminated magnetic field. The sought effect can be isolated by its dependence on the magnitude and sign of $(\omega - \omega_0)$. In this case the thermal emission of the gas and the cuvette are not substantial. The emission brilliance of a single-mode laser is so great that the effective temperature of the beam greatly exceeds the temperature of the gas, even after considerable attenuation in the cuvette.

C. Mode splitting of an optical resonator

One can propose yet another possible way of detecting a difference between $\mathrm{Re}\,\varepsilon_+$ and $\mathrm{Re}\,\varepsilon_-$. The development of laser technology has currently created an actual possibility of monitoring the intrinsic frequency of a mode of an optical resonator with an accuracy $\delta\omega \sim 10^{-4}\,\Gamma$ and even better (see, e.g.[20]), where Γ is the width of the mode. Introduction of a cuvette containing the gas to be studied inside the resonator should lead to splitting of the frequencies of dextro- and levo-polarized modes:

$$\omega_+ - \omega_- = \frac{1}{2}\omega\frac{L}{L_p}\mathrm{Re}(\varepsilon_+ - \varepsilon_-), \qquad (4.10)$$

where ω is the intrinsic frequency of the mode of the resonator without the cuvette. Here L is the length of the cuvette, and L_p is the total path length of the light in the resonator. If we use again a frequency detuning $|\omega - \omega_0| \gg \Delta\omega_D$ to diminish absorption, we get

$$\omega_+ - \omega_- = \frac{1}{2\sqrt{\pi}}\frac{c}{L_p}N\sigma_0 L\frac{\Delta\sigma}{\sigma_0}\frac{\Delta\omega_D}{\omega-\omega_0}. \qquad (4.11)$$

The width Γ of the mode of the resonator without the cuvette is determined by the losses at the mirrors, and it is

$$\Gamma = \frac{c}{2L_p}\sum_i(1 - R_i), \qquad (4.12)$$

where the R_i are the reflection coefficients of the mirrors. The concrete choice of the frequency detuning is set so that the losses due to absorption in the cuvette do not exceed the losses at the mirrors:

$$\varkappa L = \frac{1}{\sqrt{\pi}}N\sigma_0 L\frac{\gamma}{\Delta\omega_D}\frac{\Delta\omega_D^2}{(\omega-\omega_0)^2} \leqslant \sum_i(1 - R_i). \qquad (4.13)$$

The optimal frequency detuning is

$$|\omega - \omega_0| = \Delta\omega_D \sqrt{\frac{N\sigma_0 L}{\sqrt{\pi}\sum_i(1 - R_i)}\frac{\gamma}{\Delta\omega_D}}. \qquad (4.14)$$

If we substitute (4.14) into (4.11), we find

$$\frac{\omega_+ - \omega_-}{\Gamma} = \frac{1}{2\pi^{1/4}} \sqrt{\frac{N\sigma_0 L}{\sum_i (1 - R_i)} \frac{\Delta\omega_D}{\gamma} \frac{\Delta\sigma}{\sigma}}. \qquad (4.15)$$

Here we have taken account of the fact that the width Γ is twice as large as in (4.12), assuming equal losses in the cuvette and at the mirrors. We note that the size of the effect in (4.15) does not depend on N. If we assume again that $\sigma = 10^{-17}$ cm^2, $\Delta\sigma/\sigma = 2 \times 10^{-6}$, $N = 10^{18}$ cm^{-3}, $L = 200$ cm (double passage through a meter cuvette), and $\sum_i (1 - R_i) = 0.02$, we obtain from (4.14) and (4.15): $|\omega - \omega_0| = 2.4 \times 10^2 \gamma \approx 2.4 \times 10^2 \Delta\omega_D$, and $(\omega_+ - \omega_-)/\Gamma \approx 2.4 \times 10^{-4}$.

The sign of circular polarization is reversed upon reflection of the light wave from a mirror. On the other hand, the effect of non-conservation of parity must accumulate upon successive passages through the cuvette. Hence one must use either a traveling-wave ring resonator in which the wave undergoes an even number of reflections between successive passages, or a Fabry–Perot resonator in which quarter-wave plates are placed between the cuvette and the mirrors. In the latter case, the wave also retains its polarization, owing to double passage through the quarter-wave plate and reflection from the mirrors.

The scheme of the discussed experiment consists in the following (Fig. 2). Radiation from the laser L_1 with left-hand circular polarization and radiation from the laser L_2 with right-hand circular polarization are simultaneously passed through an interferometer within which a cuvette containing the studied gas is placed. An automatic-frequency-control system processes the feedback signals, which are applied to the piezoceramic laser resonators to adjust the lengths of the resonators so that the frequencies of the lasers correspond to the maxima of the transmission bands of the interferometers. Simultaneously, the beating signal from the photodetector at the frequency $\omega_+ - \omega_-$ is applied to the frequency meter. The requirements on the purity of the polarization state are not great—about the same as in the experiments to measure $\Delta\sigma/\sigma$.

We can somewhat modify the scheme of the experiment by introducing into the resonator an additional cuvette containing an optically active substance, and thus creating an additional splitting of the frequencies
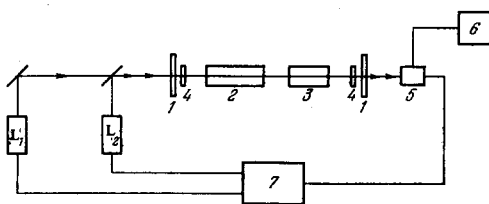

FIG. 2. Diagram of an experiment to determine the splitting of the intrinsic frequencies of an interferometer. L_1 and L_2—frequency-tunable lasers; 1—interferometer mirror, 2—cuvette containing the studied atomic gas, 3—cuvette containing an optically-active substance that produces an additional splitting of the modes of the interferometer, 4—$\lambda/4$ plates, 5—photodetector, 6—frequency meter, 7—tracking system that processes the feedback signal for tuning the frequency of the lasers.

ω_+ and ω_- that exceeds Γ. Then there is no need to ensure the polarization of the laser radiation with great accuracy. The modes ω_+ and ω_- will be excited separately when the laser frequency matches each of these frequencies, practically independently of the polarization state of the laser radiation. The studied gas will now give rise to a small frequency shift $\delta\omega_+, \delta\omega_-$ of the order of the splitting that was formerly determined by Eq. (4.15). One can isolate these shifts by using their dependence on the gas density.

Which of the two studied ways of detecting a difference between $\mathrm{Re}\,\varepsilon_+$ and $\mathrm{Re}\,\varepsilon_-$ (from the angle of rotation of the plane of polarization or the interferometric method) has the advantage will depend on the concrete experimental conditions. The difficulties of measuring rotation angles $\theta \sim 10^{-4} - 10^{-5}$ and matching of the intrinsic frequencies of a resonator ω_+ and ω_- to an accuracy of the order of $(10^{-4} - 10^{-5})\Gamma$ are apparently about the same, although they have somewhat different characteristics.

We see from the above discussion that the fundamental obstacle to attaining large effects involving $\mathrm{Re}(\varepsilon_+ - \varepsilon_-)$ is the large absorption in the studied gas. There is currently a theoretical possibility of overcoming this difficulty. It is based on the so-called phenomenon of self-induced transparency (2π-pulses), and it consists in the following (see, e.g., [27]). A pulse of resonance radiation whose duration τ is much smaller than all the relaxation times of the medium, while the amplitude $H(t)$ of the wave satisfies the condition

$$\frac{M}{\hbar} \int_{-\infty}^{\infty} H(t)\, dt = 2\pi, \qquad (4.16)$$

where M is the matrix element of the transition, can propagate in a two-level absorbing medium without losses. As we know, the reactive resonance interaction that in linear optics involves the real part of $\varepsilon(\omega)$ is conserved here. Thus, for example, one observes here an anomalously large Faraday rotation of the plane of polarization in a magnetic field that is described by practically the same formulas as in linear optics. At low intensities of the light fluxes, such a strong rotation has not been observed, owing to the strong absorption near the center of the line. One can easily show that mixing of states of different parity rotates the plane of polarization of the 2π-pulse, just like the presence of a magnetic field. In principle, the angle of rotation can be made large enough here, since the length of the cuvette can be taken to be far greater than the reciprocal of the linear absorption coefficient. However, we note that as yet the phenomenon of self-induced transparency has been observed only with not very great cuvette lengths that are less than or of the order of a tenth of the reciprocal absorption coefficient. We also note that one requires a frequency detuning of $\Delta\omega \sim \Delta\omega_D$ from the center of the line for rotation of the plane of polarization caused by non-conservation of parity. Moreover, fulfillment of the condition (4.16) requires using an extremely powerful laser pulse, since the matrix element M of the magnetic-dipole transition is about 137 times smaller than the matrix element ea_0 of the electric-dipole transition. Hence it is currently hard to make any prognoses on the 2π-pulse experiment.

5. CONCLUSION

The requirements imposed on the laser source substantially differ for the above-discussed three possible schemes for measuring effects of non-conservation of parity: 1) direct measurement of $\Delta\sigma/\sigma$, 2) measurement of the angle θ of rotation of the plane of polarization, and 3) measurement of the splitting of the intrinsic frequencies ω_+ and ω_- of an interferometer. Let us list again these requirements.

In the first experiment, one needs exact tuning of the laser frequency (within limits of $\Delta\omega_D$) to the frequency of the working transition. The requirements on the polarization state of the laser beam are not severe. There are fundamental difficulties involving the need for controlling the intensity of the light fluxes with high accuracy.

In the second and third cases, one needs only considerably cruder tuning of the laser to the defined frequency (~ 10–100 $\Delta\omega_D$).

In the third, interferometric experiment, one need not maintain with high accuracy either the intensity or the polarization state of the laser. The center of gravity is shifted to the frequency measurements. The frequency of the laser must be smoothly tunable, though indeed over a rather narrow range of the order of Γ.

In an experiment of the first type, one can use in principle either cw or pulsed lasers. In measuring the angle of rotation one can use either a cw or a pulsed laser, though it seems considerably more convenient to work with a cw laser. Finally, one can use only a cw laser for matching to the intrinsic frequencies of an interferometer.

Common to all the discussed experiments is the requirement for matching of the laser frequency to the frequency of the working transition. Currently, the frequency of laser radiation in the visible is tuned by laser action in dyes. In these generators, a dye having a broad amplification band ($\Delta\omega/\omega \sim \frac{1}{3}$) is pumped by another laser, which is cw or pulsed. The retuning of the generation frequency by the dye is carried out by changing the the parameters of the resonator.

The only continuous source for pumping a dye laser is an ionized-argon laser (several lines in the range $\lambda = 0.46$–0.51 μm). Here the dye laser frequency to be tuned overlaps the region $\lambda = 0.5$–0.8 μm. Among the elements listed in the table, transitions in cesium, rubidium, and bismuth fall in this wavelength region. As for the rest of the studied transitions in the visible, we can currently hope to tune to them only by using pulsed lasers that are retuned with dyes, and perhaps with subsequent frequency-doubling by second-harmonic generation. As pumping sources here, one can suggest the nitrogen laser, $\lambda = 0.3371$ μm (see, e.g. [21]) and the copper-vapor laser, $\lambda = 0.5105$ μm. [26]

In the infrared, tuning to the frequency of a transition currently seems to be a somewhat more complicated problem; in principle, one can hope to get stable, frequency-tunable radiation in this region by using a semi-conductor laser.

The treatment given above shows that observation in atoms of effects of non-conservation of parity caused by neutral currents in the weak interaction is a very alluring, though difficult problem. The contemporary state of quantum electronics permits us to hope for success in this very important experiment.

APPENDIX I: CALCULATION OF THE MATRIX ELEMENT OF A *P*-ODD INTERACTION

We shall take the part of the Hamiltonian for weak interaction of the electrons with the nucleus that does not conserve parity to be

$$V = -\frac{G\hbar^3}{c\sqrt{2}} Zq\frac{3}{4\pi r_0^3}\int \bar{\psi}\gamma_5\gamma_0\psi \, d\tau. \tag{I.1}$$

Here the integration of the bispinor electronic functions ψ and $\bar{\psi}$ is performed over the spherical volume of the nucleus of radius r_0. Here the density of weak charge is assumed to be uniformly distributed over the volume $(4/3)\pi r_0^3$ of the nucleus. Z is the charge of the atomic nucleus. Following [5], the factor q is assumed to be

$$q = 1 - \frac{A}{2Z} - 2\sin^2\theta, \tag{I.2}$$

A is the atomic weight of the element, $\sin^2\theta = 0.35$, and $q \approx -0.9$. In (I.1) we neglect the electron–electron part of the interaction, since the interaction of the electrons with the nucleus leads to substantially greater effects.

In the non-relativistic approximation for a point nucleus ($r_0 = 0$), the interaction (I.1) takes on the form (1.1) given in the Introduction:

$$V = -\frac{G\hbar^3}{c^2\sqrt{2}} Zq\frac{1}{2m}[(\sigma p)\,\delta(r) + \delta(r)\,(\sigma p)]. \tag{I.3}$$

Let us first study the mixing of an $s_{1/2}$ state into a $p_{1/2}$ state caused by the non-relativistic *P*-odd interaction of (I.3). The spinor wave functions of the $s_{1/2}$ and $p_{1/2}$ states having the projection of the angular momentum $j_z = \frac{1}{2}$ have the form

$$\varphi(s_{1/2}) = R_s(r)\begin{pmatrix}1/\sqrt{4\pi}\\0\end{pmatrix}, \quad \varphi(p_{1/2}) = R_p(r)\begin{pmatrix}-(1/\sqrt{3})\,Y_{10}(\theta,\varphi)\\\sqrt{2/3}\,Y_{1,1}(\theta,\varphi)\end{pmatrix}. \tag{I.4}$$

Here the $R_{s,p}(r)$ are the radial parts of the wave functions, and $Y_{10} = \sqrt{3/4\pi}\cos\theta$ and $Y_{11} = -\sqrt{3/8\pi}\sin\theta\,e^{i\varphi}$ are spherical functions. [5]

Only the second term in (I.3) contributes to the matrix element $\langle s_{1/2}|V|p_{1/2}\rangle$ of the interaction. Consequently we get

$$\langle s_{1/2}|V|p_{1/2}\rangle = -i\frac{3}{8\pi\sqrt{2}}\frac{G\hbar^4}{mc^2}ZqR_s^*(0)\left(\frac{R_p}{r}\right)_{r\to 0}. \tag{I.5}$$

Let us proceed to calculate the matrix element of the relativistic perturbation Hamiltonian of (I.1). Upon introducing the upper and lower components of the bispinor $\psi = \begin{pmatrix}\varphi\\\chi\end{pmatrix}$, we shall write the functions $\psi(s_{1/2})$ and $\psi(p_{1/2})$ in

[5] The phases of the spherical functions are taken as in [12].

the form

$$\psi(s_{1/2}) = \begin{pmatrix} f_s(r)\left(1/\sqrt{4\pi}\right) \\ 0 \\ ig_s(r)\left(-\sqrt{1/3}\,Y_{10} \atop \sqrt{2/3}\,Y_{11}\right) \end{pmatrix}, \quad \psi(p_{1/2}) = \begin{pmatrix} f_p(r)\left(-\sqrt{1/3}\,Y_{1,0} \atop \sqrt{2/3}\,Y_{1,1}\right) \\ -ig_p(r)\left(1/\sqrt{4\pi}\right) \\ 0 \end{pmatrix}.$$

(I. 6)

Upon substituting $\psi = \binom{\varphi}{\chi}$ into (I. 1) and taking (I. 6) into account, we get

$$(s_{1/2}|V|p_{1/2}) = i\frac{Gh^3}{c\sqrt{2}} Zq \frac{3}{4\pi r_0^3} \int d^3r \,[\varphi^+(s_{1/2})\chi(p_{1/2})+\chi^+(s_{1/2})\varphi(p_{1/2})]$$

$$= -i\frac{Gh^3}{c\sqrt{2}} Zq \frac{3}{4\pi r_0^3} \int_0^{r_0} r^2\,dr\,(f_s^*(r)\,g_p(r)-g_s^*(r)\,f_p(r)).$$

(I. 7)

Thus, in order to calculate the matrix element of (I. 7), we must find the relativistic radial functions within the nucleus ($r \le r_0$). The Dirac equation for the functions f and g takes on the form

$$\frac{d}{dr}(rf_\varkappa) + \frac{\varkappa}{r}(rf_\varkappa) = \frac{1}{\hbar c}(\varepsilon+2mc^2-U(r))(rg_\varkappa),$$ (I. 8a)

$$\frac{d}{dr}(rg_\varkappa) - \frac{\varkappa}{r}(rg_\varkappa) = -\frac{1}{\hbar c}(\varepsilon-U(r))(rf_\varkappa).$$ (I. 8b)

Here ε is the eigenvalue of the energy (apart from the energy mc^2), $U(r)$ is the interaction potential of the electrons with the nucleus and with the self-consistent field of the rest of the electrons of the atom, $\varkappa = -1$ for the $s_{1/2}$ state and $\varkappa = 1$ for the $p_{1/2}$ state. Analogously to what is done in the problem of the isotopic shift of atomic terms, [12,28,29] one can express the values of the functions $f_\varkappa$ and $g_\varkappa$ within the nucleus in terms of the parameters $R_s(0)$ and $(Rp(r)/r)_{r\to0}$ of the formal solution of the non-relativistic problem. Let us give the corresponding calculations.

For $r < r_0$, the potential $|U(r)| \sim Ze^2/r_0 \gg mc^2$. The coefficient $U(r)/\hbar c$ on the right-hand side of Eqs. (I. 8) is less than the centrifugal coefficient $\varkappa/r$: $|rU(r)/\hbar c| \le Z\alpha < 1$. Hence, in solving the system (I. 8) in the region $r < r_0$, we can treat the right-hand side as a perturbation. Upon introducing the new functions

$$(rf_\varkappa) = F_\varkappa(r)\,r^{-\varkappa}, \quad (rg_\varkappa) = G_\varkappa(r)\,r^{+\varkappa},$$ (I. 9)

we can formally integrate the system (I. 8):

$$F_\varkappa(r) = F_\varkappa(0) + \frac{1}{\hbar c}\int_0^r dr'\,(r')^{2\varkappa}(\varepsilon+2mc^2-U(r'))\,G_\varkappa(r'),$$ (I. 10a)

$$G_\varkappa(r) = G_\varkappa(0) - \frac{1}{\hbar c}\int_0^r dr'\,(r')^{-2\varkappa}(\varepsilon-U(r'))\,F_\varkappa(r').$$ (I. 10b)

We see from these formulas that $G_s(0) = 0$ for the $s_{1/2}$ state ($\varkappa = -1$), since otherwise the integral on the right-hand side of (I. 10a) diverges. We have $F_p(0) = 0$ for the $p_{1/2}$ state by analogous arguments. Consequently, we have the following for the wave functions, to an accuracy of first-order terms in the small parameter αZ inclusive:

$$rf_s = F_s(0)\,r, \qquad rg_s = -F_s(0)\,Z\alpha\,\frac{r^2}{r_0}\,\xi_s(r),$$

$$rf_p = G_p(0)\,Z\alpha\,\frac{r^2}{r_0}\,\xi_p(r), \quad rg_p = G_p(0)\,r.$$ (I. 11)

The positive functions $\xi_s(r)$ and $\xi_p(r)$, which have values ~ 1, are determined by the equations

$$\xi_s(r) = -\frac{1}{r^3}\frac{r_0}{Ze^2}\int_0^r U(r')\,dr',$$

$$\xi_p(r) = -\frac{1}{r^3}\frac{r_0}{Ze^2}\int_0^r [U(r')-2mc^2]\,(r')^2\,dr'.$$ (I. 12)

The matrix element of interest to us is equal to

$$(s_{1/2}|V|p_{1/2}) = -i\frac{Gh^3}{\sqrt{2}c} ZqF^*(0)\,G_p(0)\,\frac{3}{4\pi r_0^3}\int_0^{r_0} r^2\,dr\left[1+(Z\alpha)^2\frac{r^2}{r_0^2}\xi_s(r)\,\xi_p(r)\right]$$

$$\approx -i\frac{Gh^3}{\sqrt{2}c} ZqF_s^*(0)\,G_p(0)\cdot\frac{1}{4\pi}.$$

(I. 13)

In writing the second of the equations of (I. 13), we neglected the terms $\sim (Z\alpha)^2$ as compared with the terms ~ 1. In the language of wave functions, this approximation corresponds to substituting the values $g_s = 0$ and $f_p = 0$ for $r < r_0$ into the formulas of (I. 11). We note that the size of the terms that are kept in the formula (I. 13) does not depend on the type of electrostatic potential within the nucleus.

Thus we must determine the constants $F_s(0)$ and $G_p(0)$ in order to calculate the matrix element. To do this, we must find the solution of the Dirac equation outside the nucleus (for $r > r_0$) that transforms as $r \to \infty$ into the non-relativistic solutions having the needed energies and normalization, while at $r = r_0$ they satisfy the boundary conditions

$$f_s(r_0) = F_s(0), \quad g_s(r_0) = 0,$$
$$f_p(r_0) = 0, \quad g_p(r_0) = G_p(0).$$ (I. 14)

Near the nucleus, there is a rather large region in which we can neglect the shielding effect of the atomic core and the binding energy ε. In this region, the general solution of the system (I. 8) has the form

$$(rf_\varkappa) = C_\varkappa\left[(\gamma+\varkappa)\,J_{2\gamma}\left(\sqrt{\frac{8Zr}{a_0}}\right)-\frac{1}{2}\sqrt{\frac{8Zr}{a_0}}\,J_{2\gamma-1}\left(\sqrt{\frac{8Zr}{a_0}}\right)\right]$$

$$+D_\varkappa\left[(\varkappa-\gamma)\,J_{-2\gamma}\left(\sqrt{\frac{8Zr}{a_0}}\right)-\frac{1}{2}\sqrt{\frac{8Zr}{a_0}}\,J_{-2\gamma-1}\left(\sqrt{\frac{8Zr}{a_0}}\right)\right],$$

(I. 15a)

$$(rg_\varkappa) = \alpha ZC_\varkappa J_{2\gamma}\left(\sqrt{\frac{8Zr}{a_0}}\right)+\alpha ZD_\varkappa J_{-2\gamma}\left(\sqrt{\frac{8Zr}{a_0}}\right).$$ (I. 15b)

Here $C_\varkappa$ and $D_\varkappa$ are constants, $\gamma = \sqrt{\varkappa^2-(\alpha Z)^2}$, $a_0 = \hbar^2/me^2$ is the Bohr radius for hydrogen, and J_ν is the Bessel function. By equating the wave functions (I. 15) and (I. 14) at $r = r_0$, we can find expressions for $C_\varkappa$ and $D_\varkappa$ in terms of $F_s(0)$ and $G_p(0)$, in particular

$$C_s = -\Gamma(2\gamma)\,r_0\left(\frac{2Zr_0}{a_0}\right)^{-\gamma}F_s(0),$$ (I. 16a)

$$C_p = \Gamma(2\gamma)\,\frac{r_0}{\alpha Z}\left(\frac{2Zr_0}{a_0}\right)^{-\gamma}(\gamma+1)\,G_p(0).$$ (I. 16b)

In finding the coefficients $C_\varkappa$ and $D_\varkappa$, we have used the smallness of the argument of the Bessel function $(2Zr_0/a_0)^{1/2} \lesssim 0.14$ for $Z \lesssim 80$ and $r_0 = 6\times10^{-13}$ cm, and have kept only the first terms of the expansion in this parameter. The smallness of this parameter also implies that $D/C_\varkappa \sim (2Zr_0/a_0)^{2\gamma} \approx 0.01$.

In finding C_s and C_p, we note that there is a region of r values, $\alpha^6Za_0 \lesssim r \lesssim a_0Z^{-1/3}$ in which, first, the solution becomes non-relativistic, and second, we can still neglect the binding energy and the shielding effect of the atomic core. The general solution of the Schrödinger equation with an orbital angular momentum l in this region has the form $\psi = R_l(r)\,Y_{lm}(\theta,\varphi)$, where

$$R_l(r) = \widetilde{C}_l\sqrt{\frac{2Z}{a_0r}}\,J_{2l+1}\left(\sqrt{\frac{8Zr}{a_0}}\right)+\widetilde{B}_l\sqrt{\frac{2Z}{a_0r}}\,N_{2l+1}\left(\sqrt{\frac{8Zr}{a_0}}\right).$$ (I. 17)

The functions f_x from (I.15) must transform into the solution of (I.17). The arguments of the Bessel function in (I.15) and (I.17) coincide, and in the region $r \gtrsim \alpha^2 a_0 Z$, this argument is much larger than unity. Hence, we can use the asymptotic expansion of all the Bessel functions that figure in (I.15a) and in (I.17). Here we can keep in (I.15a) only the term proportional to $J_{2\gamma-1}$ (since $D_x/C_x \approx 0.01$). Matching of the amplitudes and phases of the sinusoidal oscillations of the solutions of (I.15a) and (I.17) gives

$$\tilde{C}_l = -C_x \cos[\pi(l-\gamma+1)], \quad \tilde{B}_l \approx C_x \sin[\pi(l-\gamma+1)]. \qquad (I.18)$$

The formal non-relativistic solution of the problem having a point nucleus corresponds to the case $\tilde{B}_l = 0$. We can convince ourselves of this by letting $\alpha Z \to 0$ in (I.17). Here the parameters $C_s = -\tilde{C}_s$ and $C_p = \tilde{C}_p$ determine the behavior of the non-relativistic wave functions at the coordinate origin:

$$C_s = -\frac{1}{2} \frac{a_0}{Z} R_s(0), \qquad C_p = \frac{3}{2} \frac{a_0^2}{Z^2} \left(\frac{R_p}{r}\right)_{r \to 0}. \qquad (I.19)$$

As we see from (I.17) and (I.18), the ratio $\tilde{B}_l/\tilde{C}_l = -\tan[\pi(l-\gamma+1)]$ determines the phase of the sinusoidal oscillations of the wave function, and it does not depend on the general normalization of the wave function. Matching of the logarithmic derivative of the function (I.17) (which depends only on the ratio $\tilde{B}_l/\tilde{C}_l$) with the same derivative of the solution of the Schrödinger equation in the shielding region permits one in principle to determine the position of the energy levels. The amplitude $\sqrt{\tilde{C}_l^2 + \tilde{B}_l^2}$ of the sinusoidal oscillations is determined by the normalization of the wave function. The major contribution to the normalizing integral of the wave function of an optical electron comes from the region of non-relativistic motion in the shielded Coulombic potential. Hence the amplitude $|C_x|$ of the oscillations of the wave function is practically independent of the relativistic corrections and of the corrections for the finite size of the nucleus, and we can calculate C_x by the formulas (I.19), which were written under the assumption that $\tilde{B}_l = 0$.

Combination of the formulas (I.13), (I.16a), (I.16b), and (I.19) permits us to represent the exact matrix element of the interaction of (I.1) in the form of the product of the non-relativistic matrix element of (I.5) by the correction factor λ_{rel}:

$$\langle s_{1/2} | V | p_{1/2} \rangle = \lambda_{rel} \, (-i) \frac{3}{8\pi\sqrt{2}} \frac{Gh^4}{mc^2} Z q R_s^*(0) \left(\frac{R_p}{r}\right)_{r \to 0}, \qquad (I.20)$$

$$\lambda_{rel} = \frac{2}{\Gamma^2(2\gamma)(\gamma+1)} \left(\frac{a_0}{2Zr_0}\right)^{2-2\gamma}. \qquad (I.21a)$$

We recall that this result for the relativistic correction λ_{rel} has been derived by neglecting the small additive terms of the order of $(\alpha Z)^2$. In order to get an expression for λ_{rel} with a relative accuracy including terms of the order of $(\alpha Z)^2$, we must continue the iteration in the powers of αZ in the formulas (I.11), and use the obtained wave functions in the formulas (I.13), (I.14), and (I.16). These calculations now depend on the electronic charge distribution within the nucleus, and for a constant density they give

$$\lambda'_{rel} = \frac{2}{\Gamma^2(2\gamma)(\gamma+1)} [1+0.577 (\alpha Z)^2] \left(\frac{a_0}{2Zr_0}\right)^{2-2\gamma}. \qquad (I.21b)$$

It is interesting to compare this expression with the formula for λ_{rel} obtained by Bouchiat.[5] There they calculated the relativistic correction for a (formally chosen) model of the nucleus in which the entire electric charge was concentrated at the center of the nucleus, while the entire weak charge was on the surface of the spherical nucleus of radius r_0. The calculational procedure in this model is simplified, since one uses the relativistic functions for a point Coulomb center, though it is rather hard to estimate in advance the accuracy of the calculation. The expression from[5] for λ_{rel} has the form

$$\lambda_{rel}^B = \frac{1}{\Gamma^2(2\gamma)\gamma^2} \left(\frac{a_0}{2Zr_0}\right)^{2-2\gamma}. \qquad (I.21c)$$

We can estimate the error of the formula (I.21c) by comparing it with the more exact expression (I.21b):

$$\frac{\lambda_{rel}^B}{\lambda_{rel}} = 1+0.17 \, (\alpha Z)^2. \qquad (I.21d)$$

The last equation has been written with terms of the order of $(\alpha Z)^4$ and higher neglected.

Let us proceed to discuss the parameters of the non-relativistic ψ-functions $R_s(0)$ and $(R_p/r)_{r \to 0}$. For an s-state having the principal quantum number n, we have[12]

$$|R_s(0)|^2 = 4\pi |\psi_s(0)|^2 = \frac{4Z_a^2 Z}{a_0^3 n_*^3} \left(1 + \left|\frac{\partial \Delta}{\partial n}\right|\right). \qquad (I.22)$$

Here Δ is the quantum defect, $|\partial\Delta/\partial n| \ll 1$, $n_* = \sqrt{Ry/E_s}$ is the effective principal quantum number, $Ry = me^4/2\hbar^2$; for neutral atoms $Z_a = 1$. For a hydrogen-like ion of charge Z, we should assume that $Z_a = Z$, $n_* = n$, $\partial\Delta/\partial n = 0$, and the formula (I.22) transforms into the exact formula. The applicability of this formula for polyelectronic atoms has been tested on a vast experimental material on hyperfine splitting of atomic levels.

Let us proceed as follows to determine $(R_p/r)_{r \to 0}$ (cf.[12]). The fine splitting of the $P_{1/2}$ and $P_{3/2}$ states arising from the spin-orbit interaction $V_{s-o} = (Z\alpha\hbar^3/2m^2c)r^{-3}(\mathbf{l} \cdot \mathbf{s})$ is

$$\frac{3}{2}\zeta_p = \varepsilon(P_{3/2}) - \varepsilon(P_{1/2}) = \frac{3}{2} Z\alpha^2 \, Ry \, a_0^3 \int_0^\infty r^{-3} |R_p|^2 r^2 \, dr. \qquad (I.23)$$

Here we assume that the major contribution to the splitting comes from the region of the unshielded Coulomb potential of the nucleus, for which the expression for V_{s-o} was written. In this region, the non-relativistic solution for $R_p(r)$ has the form (I.17) for $B_p = 0$. Therefore,

$$\left\langle \frac{1}{r^3} \right\rangle = \int_0^\infty r^{-1} |R_p|^2 \, dr = |\tilde{C}_p|^2 \int_0^\infty r^{-1} \frac{2Z}{a_0 r} J_3^2\left(\sqrt{\frac{8Zr}{a_0}}\right) dr = |\tilde{C}_p|^2 \frac{Z}{6a_0}. \qquad (I.24)$$

From (I.24), (I.23), and (I.19), we find

$$|R_p/r|_{r \to 0} = \frac{2}{3} \sqrt{\frac{3\zeta_p}{Ry}} \frac{Z^{1/2}}{\alpha a_0^{5/2}}. \qquad (I.25)$$

The performed calculations permit us to find the mixing coefficient β of the $n's_{1/2}$ state with the $np_{1/2}$ state:

$$\psi = \psi(np_{1/2}) + \beta\psi(n's_{1/2}),$$

$$|\beta| = \left|\frac{\langle s_{1/2} | V | p_{1/2} \rangle}{\varepsilon(p_{1/2}) - \varepsilon(s_{1/2})}\right| \qquad (I.26)$$

$$= \lambda_{rel} \frac{1}{\pi} 10^{-5} \left(\frac{m}{m_p}\right)^2 \alpha q Z_a Z^2 \frac{\sqrt{1+|\partial\Delta/\partial n|}}{n_*^{3/2}} \frac{Ry}{\Delta\varepsilon(np_{1/2}, \, n's_{1/2})} \sqrt{\frac{3\zeta_p}{2Ry}}.$$

APPENDIX II: ATOMS HAVING SEVERAL OPTICAL ELECTRONS

The operator V is an operator that is symmetrical with respect to the atomic electrons, and is of the type $\sum v$. Here the one-electron operator is a scalar product of first-order spherical tensor operators that act, respectively, on the coordinates and the spin of the electron. By using the method of genealogical coefficients and the formulas for the matrix elements of the tensor operators (see[12]), we can get

$$Q\,(l_a^n L_a S_a J;\; l_a^{n-1}\,[L_1 S_1]\,l_b S_b J)$$
$$=(-1)^{L_a+L_b+2S_a+L_1+S_1+J+3/2}\,\sqrt{6}\cdot\sqrt{n}\,G_{S_1 L_1}^{S_a L_a}\,\sqrt{(2L_a+1)\,(2L_b+1)\,(2S_a+1)\,(2S_b+1)}$$
$$\times\left\{\begin{matrix}L_a & S_a & J\\ S_b & L_b & 1\end{matrix}\right\}\left\{\begin{matrix}l_a & L_a & L_1\\ L_b & l_b & 1\end{matrix}\right\}\left\{\begin{matrix}1/2 & S_a & S_1\\ S_b & 1/2 & 1\end{matrix}\right\}.$$

(II.1)

Here the $G_{S_1 L_1}^{S_a L_a}$ are the genealogical coefficients, the formulas for the G- and $6j\left\{\begin{smallmatrix}x&y&z\\y&z&1\end{smallmatrix}\right\}$ are contained in[12], and

$$Q\,(a;\; b)=Q\,(b;\; a).$$

(II.2)

For the configurations s^2, ss, and p^5,

$$Q\,(s^2\,{}^1S_0;\; sp\,{}^3P_0)=-\sqrt{2},$$
$$Q\,(ss\,{}^1S_0;\; sp\,{}^3P_0)=-1,\quad Q\,(ss\,{}^3S_1;\; sp\,{}^1P_1)=\frac{1}{\sqrt{3}},\quad Q\,(ss\,{}^3S_1;\; sp\,{}^3P_1)=-\sqrt{\frac{2}{3}},$$
$$Q\,(p^5\,{}^2P_{3/2};\; p^4\,[{}^3P]\,s\,{}^2P_{3/2})=\frac{1}{3\sqrt{2}},$$
$$Q\,(p^5\,{}^2P_{3/2};\; p^4\,[{}^1D]\,s\,{}^2D_{3/2})=-\sqrt{\frac{5}{6}},$$
$$Q\,(p^5\,{}^2P_{1/2};\; p^4\,[{}^1S]\,s\,{}^2S_{1/2})=\frac{1}{\sqrt{3}},$$
$$Q\,(p^5\,{}^2P_{1/2};\; p^4\,[{}^3P]\,s\,{}^2P_{1/2})=-\frac{\sqrt{2}}{3}.$$

The reduced matrix elements $(a\,\|\,D\,\|\,b)$ are expressed in terms of the one-electron matrix elements by using the following formulas[12]:

$$(l_a^n L_a S_a J_a\,\|\,D\,\|\,l_a^{n-1}\,[L_1 S_1]\,l_b L_b S J_b)$$
$$=\sqrt{n}\,G_{S_1 L_1}^{SL_a}\,(-1)^{S+J_b+L_1+l_b}\,\sqrt{(2J_a+1)\,(2J_b+1)\,(2L_a+1)\,(2L_b+1)}$$
$$\times\left\{\begin{matrix}L_a & J_a & S\\ J_b & L_b & 1\end{matrix}\right\}\left\{\begin{matrix}l_a & L_a & L_1\\ L_b & l_b & 1\end{matrix}\right\}(l_a\,\|\,D\,\|\,l_b),$$

(II.3)

$$(aJ_a\,\|\,D\,\|\,bJ_b)=(-1)^{J_a-J_b}\,(bJ_b\,\|\,D\,\|\,aJ_a),$$
$$(s^2\,{}^1S_0\,\|\,D\,\|\,sp\,{}^1P_1)=\sqrt{2}\,(s\,\|\,D\,\|\,p),$$
$$(ss\,{}^3S_1\,\|\,D\,\|\,sp\,{}^3P_0)=\frac{1}{\sqrt{3}}\,(s\,\|\,D\,\|\,p),$$
$$(p^5\,{}^2P_{3/2}\,\|\,D\,\|\,p^4\,[{}^1S]\,s^2 S_{1/2})=\frac{2}{3}\,(p\,\|\,D\,\|\,s),$$
$$(p^5\,{}^2P_{3/2}\,\|\,D\,\|\,p^4\,[{}^3P]\,s\,{}^2P_{1/2})=\sqrt{\frac{2}{3}}\,(p\,\|\,D\,\|\,s),$$
$$(p^5\,{}^2P_{1/2}\,\|\,D\,\|\,p^4\,[{}^3P]\,s\,{}^2P_{3/2})=-\sqrt{\frac{2}{3}}\,(p\,\|\,D\,\|\,s),$$
$$(p^5\,{}^2P_{1/2}\,\|\,D\,\|\,p^4\,[{}^1D]\,s\,{}^2D_{3/2})=\sqrt{\frac{10}{3}}\,(p\,\|\,D\,\|\,s),$$
$$(p\,\|\,D\,\|\,s)=-(s\,\|\,D\,\|\,p)=-e\int_0^\infty R_s R_p r^3\,dr.$$

(II.4)

Here $e>0$ is the charge of the electron, and R_s and R_p are the radial functions. The formulas that relate the parameter ζ to the experimental fine-splitting values are contained in[12]. They imply that:

configuration p: $\zeta_p=\frac{2}{3}\,[E\,({}^2P_{3/2})-E\,({}^2P_{1/2})]$,

configuration p^5, $\zeta_p=-\frac{2}{3}\,[E\,({}^2P_{3/2})-E\,({}^2P_{1/2})]$,

configuration sp: $\zeta_p=2\,[E\,({}^3P_1)-E\,({}^3P_0)]$.

APPENDIX III: EXPLANATIONS FOR THE TABLE

The signs of the mixing coefficients β and of the matrix elements of the dipole moments depend on the choice of signs of the radial wave functions $R_s(r)$ and $R_p(r)$. The sign of the contribution of the corresponding transitions to the observed quantity $W_+ - W_-$ naturally does not depend on this choice. However, in order to find the sign of this contribution, we must arbitrarily fix the signs of the radial functions R_s and R_p, and calculate from these quantities both β and $(a\,\|\,D\,\|\,b)$. For determining the signs, we have used the tables of Bates and Damgaard[22] (these tables are given in the book[12]), which have the signs of the matrix elements of the dipole moments, while we took the functions R_s to be positive as $r\to\infty$. Here, for states of principal quantum number n, we have, according to the theorem on the number of zeroes of the radial function:

$$\frac{R_{ns}(0)}{|R_{ns}(0)|}=(-1)^{n+1},\quad \frac{R_{np}(r)}{|R_{np}(r)|}\bigg|_{r\to 0}=(-1)^n.$$

The value of the reduced matrix element $|(j\,\|\,D\,\|\,k)|$ $=|(k\,\|\,D\,\|\,j)|$ was recalculated from the oscillator strength $f(j,\,k)$ of the corresponding radiative transition by the formula

$$|(j\,\|\,D\,\|\,k)|^2=\frac{3}{2}\,g_j\,\frac{e^2\hbar}{m\omega_{jk}}\,f\,(j,\,k),$$

where the oscillator strength $f(j,\,k)$ is defined in such a way that $E_j>E_k$, and the probability of spontaneous emission is:

$$W_{jk}=\frac{2\omega^2 e^2}{mc^3}\,\frac{1}{g_j}\,f\,(j,\,k).$$

We shall also give the oscillator strengths of the transitions and the results of the intermediate calculations that were used in obtaining the final values given in the table.

Rubidium Rb_{85}^{37}. $\lambda_{rel}=1.55$. The lower state is admixed with the terms: $5p_{1/2}$, $|\beta|=0.225\times10^{-11}$, $f(6s_{1/2},\,5p_{1/2})=0.19$, [22] $4\chi=-1.0\times10^{-4}$; $6p_{1/2}$, $|\beta|=0.64\times10^{-12}$, $f(6p_{1/2},\,6s_{1/2})=0.52$, [22] $4\chi=0.74\times10^{-4}$. The upper state is admixed with the terms: $|\beta|=0.19\times10^{-11}$, $f(5p_{1/2},\,5s_{1/2})=0.33$, [22,23] $4\chi=-0.92\times10^{-4}$; $6p_{1/2}$, $|\beta|=0.225\times10^{-11}$, $f(6p_{1/2},\,5s_{1/2})=0.015$, [22] $4\chi=0.50\times10^{-5}$.

Cesium Cs_{133}^{55}. $\lambda_{rel}=2.5$. The lower state is admixed with the terms: $6p_{1/2}$, $|\beta|=0.117\times10^{-10}$, $f(7s_{1/2},\,6p_{1/2})=0.17$, [22] $4\chi=-4.92\times10^{-4}$; $7p_{1/2}$, $|\beta|=0.346\times10^{-11}$, $f(7p_{1/2},\,7s_{1/2})=0.48$, [22] $4\chi=+3.76\times10^{-4}$. The upper state is admixed with the terms: $6p_{1/2}$, $|\beta|=10^{-11}$, $f(6p_{1/2},\,6s_{1/2})=0.33$, [23] $4\chi=-4.78\times10^{-4}$; $7p_{1/2}$, $|\beta|=1.35\times10^{-11}$, $f(7p_{1/2},\,6s_{1/2})=10^{-3}$, [22] $4\chi=0.26\times10^{-4}$.

Strontium Sr_{88}^{38}. $\lambda_{rel}=1.55$. The lower state is admixed with the term $5s5p\,{}^3P_0$, $|\beta|=0.555\times10^{-11}$, $f(5s6s\,{}^3S_1,\,5s5p\,{}^3P_0)=0.06$, [23] $4\chi=-2.0\times10^{-4}$. The upper state is admixed with the term: $5s5p\,{}^1P_1$, $|\beta|=2.0\times10^{-11}$, $f(5s5p\,{}^1P_1,\,5s^2\,{}^1S_0)=0.51$, [23] $4\chi=-1.05\times10^{-4}$.

Barium Ba_{137}^{56}. $\lambda_{rel}=2.5$. The lower state is admixed with the term: $6s6p\,{}^3P_0$, $|\beta|=2.82\times10^{-11}$, $f(6s\,7s\,{}^3S_1,\,6s6p\,{}^3P_0)=0.17$, [23] $4\chi=3.66\times10^{-5}$. The upper state is admixed with the term: $6s6p\,{}^1P_1$, $|\beta|=1.03\times10^{-11}$, $f(6s6p\,{}^1P_1,\,6s^2\,{}^1S_0)=0.47$, [23] $4\chi=-1.86\times10^{-5}$.

Mercury Hg_{200}^{80}. $\lambda_{rel} = 6.1$. The lower state is admixed with the term: $6s6p\,^3P_0$, $|\beta| = 1.28 \times 10^{-10}$, $f(6s7s\,^3S_1,\ 6s6p\,^3P_0) = 0.07$,[23] $4\chi = 4.3 \times 10^{-5}$. The upper state is admixed with the term: $6s6p\,^1P_1$, $|\beta| = 1.16 \times 10^{-10}$, $f(6s6p\,^1P_1,\ 6s^2\,^1S_0) = 0.4$,[23] $4\chi = -6.0 \times 10^{-5}$.

Iodine I_{127}^{53}, $\lambda_{rel} = 2.36$. The lower state is admixed with the terms:[6] $5p[^3P]6s\,^2P_{3/2}$, $|\beta| = 0.18 \cdot 10^{-11}$; $5p^4[^1D]6s\,^2D_{3/2}$ $|\beta| = 1.1 \cdot 10^{-11}$. The upper state is admixed with the terms $5p^4[^3P]6s\,^2P_{1/2}$, $|\beta| = 0.36 \cdot 10^{-11}$, $5p^4[^1S]6s''\,^2S_{1/2}$, $|\beta| = 0.45 \cdot 10^{-11}$. The oscillator strengths of the admixed transitions were estimated[24]: $f \sim 0.15$. The relative signs of the contributions of the corresponding transitions could not be established. Hence the value of 4χ given in the table corresponds to the contribution of the only admixed $5p^4[^1D]6s\,^2D_{3/2}$.

tor strengths of the admixed transitions were estimated in[24]: $f \sim 0.15$. The relative signs of the contributions of the corresponding transitions could not be established. Hence the value of 4χ given in the table corresponds to the contribution of the only admixed state $5p^4[^1D]6s \times\,^2D_{3/2}$.

Thallium Tl_{204}^{81}. $\lambda_{rel} = 6.1$. The lower state is admixed with the term: $7s_{1/2}$, $|\beta| = 0.86 \times 10^{-10}$, $f(7s_{1/2},\ 6p_{3/2}) = 0.28$,[23] $4\chi = -2.63 \times 10^{-7}$.

Lead Pb_{207}^{82}. $\lambda_{rel} = 6.1$. The lower state is admixed with the term: $6p7s\,^3P_0$, $|\beta| = 0.9 \times 10^{-10}$, $f(6p7s\,^3P_0,\ 6p^2\,^3P_1) \sim 5.10$,[24] $4\chi \sim 1.3 \times 10^{-6}$. The upper state is admixed with the term: $6p7s\,^3P_1$, $|\beta| \sim 1.0 \times 10^{-10}$, $f(6p7s\,^3P_1,\ 6p^2\,^3P_0) \sim 5.10^{-2}$,[24] $4\chi \sim 1.0 \times 10^{-6}$. An intermediate type of coupling occurs in this element. Hence ζ_p from (I.26) was taken to be $\zeta_p = 7290$ cm^{-1} according to[17]. The values of β and the oscillator strengths were estimated very crudely without accounting for the Q-factors.

Bismuth Bi_{209}^{83}. $\lambda_{rel} = 6.1$. An intermediate type of coupling occurs, $\zeta_p = 10.100$ cm^{-1}.[17] Reliable calculation of the oscillator strengths and Q-factors is difficult. Hence we took for all the admixed terms the averaged estimate $|\beta| \sim 2 \times 10^{-10}$, $f \sim 10^{-1}$.

In conclusion, we note that a more exact calculation of the parameter χ is a rather unwieldy procedure; such a calculation can be expediently undertaken only in connection with experiments performed on a concrete element.

---

[6]The notation of the terms and their energies are taken from[25].

---

[1]E. Condon, Phys. Rev. 49, 459 (1936).

[2]I. E. Tamm, Dokl. Akad. Nauk SSSR 21, 106 (1938): also Sobranie Nauchnyhk trudov (Collected Scientific Works), Vol. 1, Nauka, m., 1975, p. 320.

[3]Ya. B. Zel'dovich, Zh. Eksp. Teor. Fiz. 36, 964 (1959) [Sov. Phys. JETP 9, 682 (1959)].

[4]F. C. Michel, Phys. Rev. B138, 408 (1965).

[5]M. Bouchiat and C. Bouchiat, Phys. Lett. B48, 111 (1974); J. de Phys. 35, 899 (1974).

[6]A. N. Moskalev, Pis'ma Zh. Eksp. Teor. Fiz. 19, 394 (1974) [JETP Lett. 19, 216 (1974)].

[7]Ya. A. Azimov, A. A. Ansel'm, A. N. Moskalev, and R. M. Ryndin, Zh. Eksp. Teor. Fiz. 67, 17 (1974) [Sov. Phys. JETP 40, 8 (1975)].

[8]I. B. Khriplovich, Yad. Fiz. 21, 1046 (1975) [Sov. J. Nucl. Fiz. 21, 538 (1975)].

[9]I. B. Khriplovich, Pis'ma Zh. Eksp. Teor. Fiz. 20, 686 (1974) [JETP Lett. 20, 315 (1974)].

[10]V. G. Gorshkov and L. N. Labzovskii, *ibid.* 19, 768 (1974) [JETP Lett. 19, 394 (1974)].

[11]A. N. Moskalev, R. M. Ryndin, and I. B. Khirplovich, Usp. Fiz. Nauk. 118, 409 (1976) [Sov. Phys. Usp. 19, 220 (1976)].

[12]I. I. Sobel'man, Vvedenie v teoriyu atomnykh spektrov (Introduction to the Theory of Atomic Spectra), Fizmatgiz., M., 1963 (Engl. Transl., Pergamon Press, Oxford, 1972).

[13]G. W. F. Drake, Phys. Rev. A3, 908 (1971).

[14]I. L. Beigman and U. I. Safronova, Zh. Eksp. Teor. Fiz. 60, 2045 (1971) [Sov. Phys. JETP 33, 1102 (1971)].

[15]L. A. Vainshtein and V. N. Shevel'ko, Opisanie programmy dlya rascheta atomnykh kharakteristik (Description of a Program for Calculating Atomic Characteristics). Preprint of the Institute of Physics of the Academy of Sciences of the USSR No. 26, Moscow, 1974.

[16]Fizicheskie protsessy v gazovykh tumannostyakh (Physical Processes in Gaseous Nebulae), Gostekhizdat, M., 1948.

[17]H. A. Robinson and G. H. Shortley, Phys. Rev. 52, 713 (1937).

[18]I. L. Beigman, Opt. Spektrosk. 99, 999 (1963).

[19]V. N. Faddeeva and N. M. Terent'ev, Tablitsy znachenii integrala veroyatnosti ot kompleksnogo argumenta (Tables of values of the Probability Integral for Complex Argument), Gostekhizdat, M., 1954.

[20]J. Levine and J. L. Hall, J. Geophys. Res. 77, 2595 (1972).

[21]R. V. Ambartsumyan, G. I. Bekov, V. S. Letokhov, and V. I. Mishin, Pis'ma Zh. Eksp. Teor. Fiz. 21, 595 (1975). [JETP Lett. 21, 279 (1975)].

[22]D. R. Bates and A. Damgaard, Phil. Trans. 242, 101 (1949).

[23]S. E. Frish, Opticheskie spektry atomov (Optical Spectra of Atoms), Fizmatgiz, M.-L., 1963.

[24]L. A. Vainshtein, I. I. Sobel'man, and E. A. Yukov, Secheniya vozbuzhdeniya atomiv i ionov élektronami (Cross-sections for Excitation of Atoms and Ions by Electrons), Nauka, M., 1973.

[25]C. E. Moore, Atomic Energy Levels, v. I–III, Nat. Bur. Stand. USA, 1952, 1958, 1971.

[26]A. A. Isaev, M. A. Kazaryan, and G. G. Petrash, Pis'ma Zh. Eksp. Teor. Fiz. 16, 40 (1972) [JETP Lett. 16, 27 (1972)].

[27]M. A. Poluektov, Yu. M. Popov, and V. S. Roitberg, Usp. Fiz. Nauk 114, 97 (1974); Kvantovaya Elektron. (Moscow) 1, 757, 1309 (1974) [Sov. Phys. Usp. 17, 673 (1975); Sov. J. Quantum Electron. 4, 423, 719 (1974)].

[28]G. Racah, Nature, 129, 723 (1932).

[29]J. E. Rosenthal and G. Breit, Phys. Rev. 41, 459 (1932).

Translated by M. V. King